PASJ: Publ. Astron. Soc. Japan , 1–??,

Non-Equilibrium Ionization State and Two-Temperature Structure in the Linked Region of Abell 399/401

Takuya Akahori and Kohji Yoshikawa
Center for Computational Sciences, University of Tsukuba, 1-1-1, Tennodai, Tsukuba, Ibaraki 305-8577
akataku@ccs.tsukuba.ac.jp, kohji@ccs.tsukuba.ac.jp

(Received 2008 May 16; accepted 2008 June 2)

Abstract

We investigate a non-equilibrium ionization state and two-temperature structure of the intracluster medium in the linked region of Abell 399/401, using a series of N-body + SPH simulations, and find that there exist significant shock layers at the edge of the linked region, and that the ionization state of iron departs from the ionization equilibrium state at the shock layers and around the center of the linked region. As for the two-temperature structure, an obvious difference of temperature between electrons and ions is found in the edge of the linked regions. Kα line emissions of Fe XXIV and Fe XXV are not severely affected by the deviation from the ionization equilibrium state around the center of the linked region, suggesting that the detection of relatively high metallicity in this area cannot be ascribed to the non-equilibrium ionization state of the intracluster medium. On the other hand, the Kα emissions are significantly deviated from the equilibrium values at the shock layers, and the intensity ratio of Kα lines between Fe XXIV–XXV and Fe XXVI is found to be significantly altered from that in the ionization equilibrium state.

Key words: galaxies: intergalactic medium — X-rays: galaxies: clusters — X-rays: individual (A 399, A 401)

1. Introduction

According to a standard scenario of hierarchical structure formation in the universe, galaxy clusters are formed through successive merging of galaxies, galaxy groups, and clusters. About a half of observed clusters have irregular X-ray morphology (e.g., Akahori, Masai 2005 references therein), and a part of such irregularities thought to be caused by such merging events.

Abell 399/401 is well-known as merging clusters on an early stage of the merging. Fujita et al. (1996) and Sakelliou, Ponman (2004) found that the intracluster medium (ICM) at the linked region of the two clusters is compressed based on the ASCA and XMM-Newton observations, respectively. Recently, Fujita et al. (2008) reported the detection of Fe K emission lines near the center of the linked region based on the Suzaku XIS observation, and the metallicity in that regions is estimated to be 0.2 times the solar metallicity, which seems relatively high compared with theoretical predictions based on numerical simulations (e.g., Tornatore et al. 2007).

The estimation of physical properties of ICM in X-ray observations is usually based on the assumptions that ICM is in the ionization equilibrium state and that electrons and ions share the same thermal temperature. Such assumptions can be justified around central regions of galaxy clusters by the fact that ICM density is high enough to quickly achieve ionization equilibrium and thermal equilibration between electrons and ions. As for the ionization equilibrium, the timescale required to reach collisional ionization equilibrium for an ionizing plasma, is estimated as $n_e t \gtrsim 10^{12}$ cm^{-3} s (see e.g., Masai 1984), where n_e is the number density of electrons. Therefore, for $n_e \sim 10^{-4}$ cm^{-3} in the linked region (Sakelliou, Ponman 2004; Fujita et al. 2008), $t \sim$ Gyr is comparable to or longer than the merger timescale, so that the ionization equilibrium is no longer a reasonable assumption. Actually, in the warm-hot intergalactic medium (WHIM), where the density is much lower, the deviation from the ionization equilibrium have been pointed out by Yoshikawa, Sasaki (2006). In addition, the thermal equilibration in merging clusters has been studied by Takizawa (1999) based on N-body/SPH simulations, and the two-temperature structure of ICM, i.e. the difference in temperature between electrons and ions, is reported especially at low-density regions. The two-temperature structure of WHIM has been also suggested by Yoshida et al. (2005).

Therefore, there exists sufficient reasons to suspect that these assumptions are not valid in the linked region of Abell 399/401. In this paper, we investigate an ionization state and temperature structure of ICM in the linked region by relaxing the assumptions of ionization equilibrium and thermal equipartition between electrons and ions, and verify to what extent such a non-equilibrium state affect the interpretations of the observational data.

2. Model and Calculation

We carry out N-body/SPH simulations of two merging galaxy clusters, in which a non-equilibrium ionization state and two-temperature structure of ICM are both taken into account. Radiative cooling and electron heat

conduction are both ignored in these simulations.

The time evolution of two-temperature structure is followed with the same way as Takizawa (1999). We assume that the electrons and ions always reach Maxwellian distributions with temperatures, $T_{\rm e}$ and $T_{\rm i}$, respectively, and the two temperatures are equalized through Coulomb scattering on a timescale of

$$t_{\rm ei} = 2\times10^8 \ {\rm yr} \frac{(T_{\rm e}/10^8 \ {\rm K})^{3/2}}{(n_{\rm i}/10^{-3} \ {\rm cm}^{-3})} \cdot \left(\frac{40}{\ln\Lambda}\right), \quad (1)$$

where $n_{\rm i}$ is the number density of ions, and $\ln\Lambda$ is the Coulomb logarithm. By introducing the dimensionless temperatures of electrons and ions, $\tilde{T}_{\rm e} \equiv T_{\rm e}/T$ and $\tilde{T}_{\rm i} \equiv T_{\rm i}/T$, respectively, normalized by the mean temperature of electrons and ions, $T \equiv (n_{\rm e}T_{\rm e} + n_{\rm i}T_{\rm i})/(n_{\rm e}+n_{\rm i})$, the evolution of two-temperature structure is described by

$$\frac{d\tilde{T}_{\rm e}}{dt} = \frac{\tilde{T}_{\rm i} - \tilde{T}_{\rm e}}{t_{\rm ei}} - \frac{\tilde{T}_{\rm e}}{u} Q_{\rm sh}, \quad (2)$$

where u and $Q_{\rm sh}$ are the specific thermal energy and the shock heating rate per unit mass, respectively. The first term of the r.h.s. denotes the thermal relaxation rate between ions and electrons. Note that recent studies on supernova remnants showed that $T_{\rm e}/T_{\rm i} \sim 1$ around the shock for relatively small Mach numbers (Ghavamian et al. 2007); electrons may be heated by some plasma waves. However, for a cluster merger, the Mach number of the shock is 'very' small (< 5). In this case, waves may not be generated and electrons may not be heated. In this letter, we ignore the effect of electron heating by plasma waves.

The time evolution of ionization fractions of ions is computed by solving

$$\frac{df_j}{dt} = \sum_{k=1}^{j-1} S_{j-k,k} f_k - \sum_{i=j+1}^{Z+1} S_{i-j,j} f_j - \alpha_j f_j + \alpha_{j+1} f_{j+1}, \quad (3)$$

where j is the index of a particular ionization stage considered, Z the atomic number, f_j the ionization fraction of an ion j, $S_{i,j}$ the ionization rate of an ion j with the ejection of i electrons, and α_j is the recombination rate of an ion j. Ionization processes include collisional, Auger, charge-transfer, and photo-ionizations, and recombination processes are composed of radiative and dielectronic recombinations. Ionization and recombination rates are calculated by utilizing the SPEX ver 1.10 software package[1]. Actual calculations are carried out in essentially the same way as Yoshikawa, Sasaki (2006), except that the reaction rates are computed using the electron temperature, $T_{\rm e}$, rather than the mean temperature, T, in order to incorporate the effect of two-temperature structure. We solve the time evolution of each ionization fraction of H, He, C, N, O, Ne, Mg, Si, S, and Fe, but we focus only on iron.

To reproduce the situation of Abell 399/401, the initial condition of the two clusters is set up as follows. We consider a head-on merger (Oegerle, Hill 1994), and assume that their collision axis is perpendicular to the line of sight. Each cluster has the same shape for simplicity since the differences of the two clusters in shape and size are slight (Sakelliou, Ponman 2004). We adopt the King profile for the initial dark matter distribution, in which the radial velocity dispersion, σ_{*r}, satisfies $\sigma_{*r}^2 = k_{\rm B}T_{\rm vir}/\mu m$, where $k_{\rm B}$ is the Boltzmann constant and $T_{\rm vir}$ is the virial temperature (the virial radius is $r_{\rm vir} = 3.0$ Mpc and the cluster mass is $M(r_{\rm vir}) \simeq 1.7\times10^{15} \ M_\odot$). For the initial ICM distribution, we first assume the temperature profile, $T(r) = (T_{\rm vir}/\beta)\exp(-r/r_{\rm vir})$, with $\beta = 0.6$, and the density profile is obtained by assuming hydrostatic equilibrium. The above parameters are chosen so that X-ray surface brightness satisfies the β-model best-fit (Sakelliou, Ponman 2004), and that the spectroscopic-like temperature, $T_{\rm sl}$ (Mazzotta et al. 2004), reproduces the observed temperature at the unperturbed regions by Markevitch et al. (1998). The number of particles of each galaxy cluster is set to a half million each for dark matter and ICM. The initial relative velocity of the two clusters is set to 1050 km/s to reproduce the observed temperature of the linked region in terms of $T_{\rm sl}$, and the initial separation is ~ 7 Mpc. As for the metallicity, a spatially uniform metallicity of 0.2 times the solar abundance is assumed. It should be noticed that the metallicity, Z, is very insensitive to the resulting ionization state of ions as long as $Z \ll 1$. We also assume $\tilde{T}_{\rm e} = \tilde{T}_{\rm i} = 1$ and an ionization equilibrium state at the start of the simulation.

3. Result

In the rest of this paper, we present the results of a snapshot of the simulation in which the separation between the centers of the two clusters is ~ 3 Mpc so that their configuration is consistent with that of Abell 399/401. Figure 1a–1e show physical properties on a cross section along the collision axis of the two clusters. The white-solid square with 1.5 Mpc on a side shows the region roughly corresponding to the observed area by Fujita et al. (2008). In this region, the local ICM density, n $(= n_{\rm e} + n_{\rm i}) \sim 3\times10^{-4}$ cm^{-3} (figure 1a), and $T_{\rm sl} = 6.48$ keV are in good agreement with the observations (Sakelliou, Ponman 2004; Fujita et al. 2008).

We find that the shock heating rate is typically a few percent of the adiabatic heating rate inside the linked region. This means that both the electrons and ions are mainly heated by the adiabatic compression in almost the same rate with no significant shocks there. Accordingly, as can be seen in figure 1c, the electron temperature is only a few percent lower than the mean temperature in this region. On the other hand, at the edge of the linked region (the white-dashed rectangles), there exist significant shock layers with mach number of 1.5–2. In these layers, we can see that the electron temperature is typically 10–20 % lower than the mean temperature, and even lower toward outer regions.

Figure 1d and 1e show the ionization fraction of Fe XXV and the ratio of the fraction relative to that in the ionization equilibrium state, respectively. Here, the ionization equilibrium state is calculated assuming that $T_{\rm e} = T_{\rm i}$. In

[1] http://www.sron.nl/divisions/hea/spex/

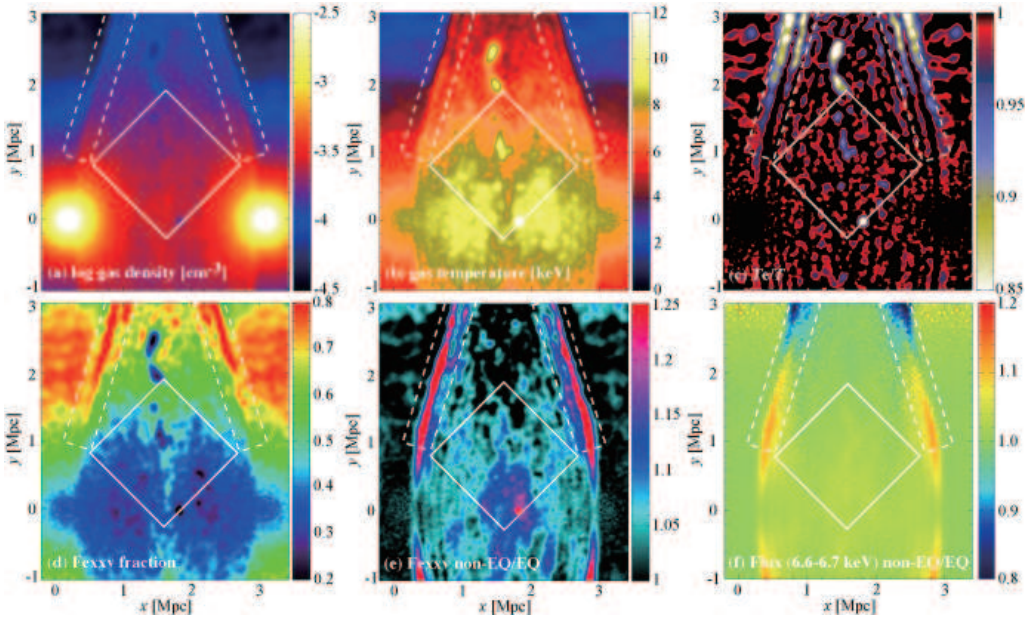

Fig. 1. Maps of (a) the ICM density in units of log cm^{-3}, (b) the mean temperature in keV, (c) the ratio of the electron temperature relative to the mean temperature, (d) the ionization fraction of Fe XXV, (e) the ratio of the Fe XXV fraction relative to that in the ionization equilibrium state, and (f) the ratio of the line intensity in 6.6–6.7 keV band integrated along the line of sight relative to that in the equilibrium state. The white-solid squares and white-dashed rectangles indicate the regions corresponding to the Suzaku observation by Fujita et al. (2008) and the shock layers, respectively.

the center of the linked region, the Fe XXV fraction is typically 30–60 %, the largest among other ionization states, and is 10–20 % larger than that in the equilibrium state. In the shock layers at the edge of the linked region, the Fe XXV fraction is nearly 80 % and 30–40 % larger than that in the ionization equilibrium state.

The excess of the Fe XXV fraction can be understood as follows. In the linked region, the electron temperature is increasing from ~ 3 keV to ~ 8 keV according to the adiabatic compression and/or the shock heating, so that the Fe XXV fraction is decreasing in time because an Fe XXV fraction peaks at ~ 3 keV and decreases as the temperature increases in the ionization equilibrium state. However, the ionization of Fe XXV to higher ionization states is not quick enough to catch up with the ionization equilibrium state, leaving the Fe XXV fraction larger than that in the equilibrium state.

Deviations from the ionization equilibrium state can be seen also for Fe XXIV. Its fraction is $\simeq 2$–3 %, and ~ 15–20 % larger than that in the equilibrium state. Due to the excess of Fe XXIV and Fe XXV fractions, the fractions of Fe XXVI and Fe XXVII are ~ 5 % and ~ 15–20 % smaller than those in the equilibrium state, respectively.

As a result of the deviation from the ionization equilibrium, the intensities of iron line emissions are altered to some extent. We calculate X-ray spectrum from the simulation using the SPEX package, and find that Kα lines of Fe XXIV and Fe XXV in a rest-frame energy band of 6.6–6.7 keV is larger than those in the ionization equilibrium state, primarily because of the excess of Fe XXV fraction. On the other hand, since the Fe XXVI fraction is smaller than that in the equilibrium state, Kα lines of Fe XXVI in 6.9–7.0 keV band in rest frame are dimmer. It should be noted that the iron line emission detected in Fujita et al. (2008) corresponds to the Kα lines of Fe XXIV and Fe XXV in the 6.6–6.7 keV energy band. Figure 1f depicts the ratio of the intensity in 6.6–6.7 keV band projected along the line of sight relative to that in the ionization equilibrium state, and it can be seen that the intensity changes are significant (typically ~ 15 %) at the shock layers, while the intensity is only a few percent enhanced around the area of the Suzaku observation by Fujita et al. (2008), despite the excess of the Fe XXV fraction by 10–20 % (figure 1e). This is because the deviation from the ionization equilibrium is significant only at the center of the linked region, and its effect is diluted in integrating along the line of sight. This suggests that the iron line emission detected by Fujita et al. (2008) is not severely affected by the deviation from the ionization equilibrium. Here, let us define the ratio of the X-ray intensity between the two energy bands as

$$R = \frac{F(6.6-6.7\ \mathrm{keV})}{F(6.9-7.0\ \mathrm{keV})}. \quad (4)$$

Figure 2 shows the map of the ratio $R/R_{\rm eq}$, where $R_{\rm eq}$ is the intensity ratio defined above but in the ionization equilibrium state, and clearly indicates that the intensity ratio departs from the one in the ionization equilibrium state within the shock layers. Note that this intensity ratio is independent of the local abundance of iron, but primarily depends on its ionization state. Therefore, such excess of the intensity ratio, R, can be used as a stringent observational tracer of the non-equilibrium ionization state.

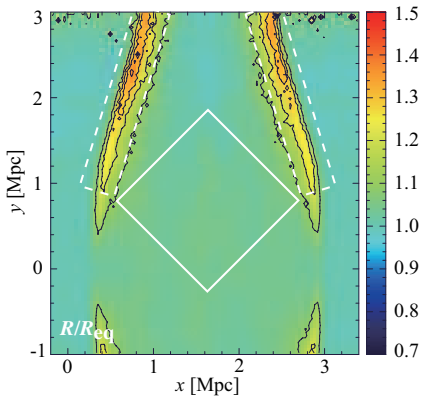

Fig. 2. The map of the ratio, $R/R_{\rm eq}$, in the same region as figure 1. The contours from outside to inside indicate $R/R_{\rm eq} = 1.1$ to 1.4 separated by a difference of 0.1.

4. Conclusion and Discussion

The ionization state of iron and two-temperature structure in the linked region of Abell 399/401 is investigated by using N-body + SPH simulations by relaxing the assumptions of ionization equilibrium and thermal equilibration between electrons and ions.

It is found that, around the center of the linked region, the Fe XXV fraction is 10–20 % larger than that in the ionization equilibrium state, and the electron temperature is only a few percent smaller than the mean temperature of electrons and ions, because the ICM is mainly adiabatically heated inside the linked region. On the other hand, we find that there exist shock layers at the edge of the linked region, and that the Fe XXV fraction is larger than that in the ionization equilibrium state by 30–40 %, and the electron temperature is typically 10–20 % lower than the mean temperature around these layers.

Our simulation indicates that the intensity of Fe Kα emission lines is affected by such deviation from the ionization equilibrium state of iron in the linked region. While the deviation from the ionization equilibrium state is remarkable around the center and the edge of the linked region, we find that the emission line intensity is strongly affected preferentially at the edge of the linked region.

The area of the Suzaku XIS observation by Fujita et al. (2008), in which fairly high metallicity is reported, is located at the central portion of the linked region. Our results imply that X-ray emission in this area is not strongly affected by the effects of a non-equilibrium ionization state and two-temperature structure. Therefore, the fact that high metallicity is detected in this area cannot be ascribed to the non-equilibrium ionization state of the ICM, and must be explained by other physical processes.

It is interesting to discuss the detectability of the non-equilibrium ionization state and the two-temperature structure of ICM in Abell 399/401. According to our simulations, it is expected that shock layers with a mach number of 1.5–2 are located at the edge of the linked region, and that the ratio between Kα emission lines of Fe XXIV–XXV and Fe XXVI are significantly different from that in the ionization equilibrium state. Observationally, such an intensity ratio of iron emission lines could be important clues for the detection of the deviation from the ionization equilibrium in these layers. In principle, the indication of the two-temperature structure can be also obtained by the difference between electron and ion temperatures inferred from X-ray thermal continuum and thermal width of emission lines, respectively. Of course, the detections of the non-equilibrium ionization state and the two-temperature structure are not very feasible with the current observational facilities, but could be achieved by the X-ray spectroscopy with a high energy resolution using X-ray calorimeters in near future.

Finally, we should discuss several caveats on the assumptions adopted in this work. The slope of the density profile, i.e. β, is a sensitive parameter to the non-equilibrium ionization state and two-temperature structure. If we adopt $\beta = 0.5$, the resultant departure from the ionization equilibrium is suppressed because the ICM density at the outskirts is relatively denser and the equilibration timescales become shorter. In addition, we assume that the encounter is taking place on the plane of the sky. If it is not the case, the effect of the non-equilibrium ionization state on the observed X-ray intensity at the shock layers would be blurred to some extent in integrating along the line of sight, depending on the viewing angle.

The authors would like to thank an anonymous referee for useful comments and suggestions. This work is carried out with computational facilities at Center for Computational Sciences in University of Tsukuba, and supported in part by Grant-in-Aid for Specially Promoted Research (16002003) from MEXT of Japan, and by Grant-in-Aid for Scientific Research (S) (20224002) and for Young Scientists (Start-up) (19840008) from JSPS.

References

Akahori, T., & Masai, K. 2005, PASJ, 57, 419
Fujita, Y., Koyama, K., Tsuru, T., & Matsumoto, H., 1996, PASJ, 48, 191
Fujita, Y., Tawa, N., Hayashida, K., Takizawa, M., Matsumoto, H., Okabe, N., & Reiprich, T. H. 2008, PASJ, 60, S343
Ghavamian, P., Laming, J. M., & Rakowski, C. E. 2007, ApJL, 654, L69
Haardt, F., & Madau, N. Y. 2001, astro-ph/0106018
Markevitch, M., Forman, W. R., Sarazin, C. L., & Vikhlinin, A. 1998, ApJ, 503, 77
Masai, K. 1984, Ap&SS, 98, 367
Mazzotta, P., Rasia, E., Moscardini, L., & Tormen, G. 2004, MNRAS, 354, 10
Oegerle, W. R., & Hill, J. M. 1994, AJ, 107, 857
Sakelliou, I., & Ponman, T. J. 2004, MNRAS, 351, 1439
Takizawa, M. 1999, ApJ, 520, 514
Tornatore, L., Borgani, S., Dolag, K., & Matteucci, F. 2007, MNRAS, 382, 1050
Yoshida, N., Furlanetto, S. R., & Hernquist, L. 2005, ApJ, 618, L91
Yoshikawa, K., & Sasaki, S. 2006, PASJ, 58, 641